Neurosci. Bull. June, 2019, 35(3):369–377
https://doi.org/10.1007/s12264-018-0291-x

www.neurosci.cn
www.springer.com/12264

REVIEW

Illuminating the Activated Brain: Emerging Activity-Dependent Tools to Capture and Control Functional Neural Circuits

Qiye He[1,2] · Jihua Wang[1] · Hailan Hu[1,2]

Received: 27 March 2018 / Accepted: 13 June 2018 / Published online: 26 September 2018

Abstract Immediate-early genes (IEGs) have long been used to visualize neural activations induced by sensory and behavioral stimuli. Recent advances in imaging techniques have made it possible to use endogenous IEG signals to visualize and discriminate neural ensembles activated by multiple stimuli, and to map whole-brain-scale neural activation at single-neuron resolution. In addition, a collection of IEG-dependent molecular tools has been developed that can be used to complement the labeling of endogenous IEG genes and, especially, to manipulate activated neural ensembles in order to reveal the circuits and mechanisms underlying different behaviors. Here, we review these techniques and tools in terms of their utility in studying functional neural circuits. In addition, we provide an experimental strategy to measure the signal-to-noise ratio of IEG-dependent molecular tools, for evaluating their suitability for investigating relevant circuits and behaviors.

Keywords Immediate-early gene · Emotion · Activity-dependent tools · Neural ensembles · c-fos · Arc

✉ Qiye He
qhe@zju.edu.cn

✉ Hailan Hu
huhailan@zju.edu.cn

[1] Center for Neuroscience, and Department of Psychiatry of First Affiliated Hospital, NHC and CAMS Key Laboratory of Medical Neurobiology, Zhejiang University School of Medicine, Hangzhou 310058, China

[2] Interdisciplinary Institute of Neuroscience and Technology, Qiushi Academy for Advanced Studies, Zhejiang University, Hangzhou 310012, China

Introduction

One of the most intriguing problems in neuroscience is to understand how brains respond to various sensory and behavioral stimuli [1, 2]. At the cellular level, these stimuli are represented (i.e. encoded) by specific stimulus-activated neural ensembles. Visualizing and manipulating these ensembles in lab animals will allow us to reveal the neural circuits and underlying neural mechanisms that drive specific behavioral responses, which will ultimately be used to understand the neuroscience of human behaviors and the neuropathology of related disorders.

Immediate-early genes (IEGs) such as *c-fos*, *Arc*, and *Zif268/Egr1* are rapidly activated in stimulated neurons [3–5], and IEG activation has long been used to label and map stimuli-activated neural ensembles by direct visualization through either immunohistochemistry (IHC) or *in situ* hybridization (ISH) [6, 7]. Additional co-staining for markers of specific neuronal types has further revealed the cellular identities of activated neural ensembles, and has provided the foundation for using the molecular tools described below to trace the circuits activated by stimuli.

In recent years, novel techniques have been developed to further expand the application of IEGs to the study of the neural activation patterns induced by various types of stimuli or behavioral experiences. In this review, we first focus on novel imaging techniques that use endogenous IEG signals to either differentiate neural ensembles activated by multiple stimuli, or to visualize activated neural networks at the whole-brain scale and single-neuron resolution. Then we discuss novel tools that use IEG-based regulatory sequences or molecules modulated by Ca^{2+}-influx to label and manipulate neurons and their projections.

Dual-Epoch Mapping Techniques to Discriminate Different Functional Circuits

It is often desirable to map the neural representations of two distinct stimuli, such as emotional stimuli of an appetitive and an aversive nature [8–13], across the whole brain at single-cell resolution. This naturally raises the question of whether the same neural ensemble is activated by both stimuli. Experimentally, a single ISH or IHC against an IEG in a dual-stimulated test animal cannot differentiate the two ensembles. Neither can this be done by comparing the neural activation patterns between two test animals, each given one of the stimuli, due to the inherent variability in the spatial distribution of neurons between animals.

To solve this problem, several labs have developed IEG-dependent dual-epoch mapping techniques to identify and differentiate neural ensembles activated by different stimuli in the brain of the same animal. Cellular compartment analysis of temporal activity by fluorescence *in situ* hybridization (CatFISH) was developed to visualize and distinguish the hippocampal neural ensembles activated by different environments using experience-induced *Arc* (activity-regulated cytoskeleton-associated) mRNA [14, 15]: in CatFISH, the test animals are first placed in a novel environment for 5 min, returned to their home cages for ~20 min, and then placed in a second novel environment for 5 min before being sacrificed. The 20-min interval between the two novel environments allows the *Arc* mRNA induced by the first novel environment to be completely transported out of the nucleus to the cytoplasm, while by the time the test animals are sacrificed, the *Arc* mRNA induced by the second environment remains exclusively in the nucleus. Thus, neural ensembles activated by different environments can be distinguished by the subcellular distribution of *Arc* mRNA. Based on similar principles, a *c-fos*-based CatFISH was later developed to label neurons activated by mating and fighting behaviors in mice [16].

Alternatively, several groups developed a differential-labeling technique separately using the mRNA and protein signals of the same IEG. This is based on the finding that the mRNA signals of IEGs such as *c-fos* and *zif268/Egr1* rise and peak very rapidly in stimulus-activated neurons, but their protein signals accumulate and peak significantly later. Such differences in the kinetics of mRNA and protein accumulation lead to a substantial temporal separation between the stimuli-induced mRNA and protein peaks (Fig. 1). So, when two stimuli separated by an appropriate time interval are applied to the same animal, at a carefully chosen time point of inspection, the IEG signals in neurons activated by the first stimulus will all be in protein form, while those in neurons activated by the second stimulus will all be in mRNA form. Thus, the two differently-activated neural ensembles can be distinguished using ISH and IHC.

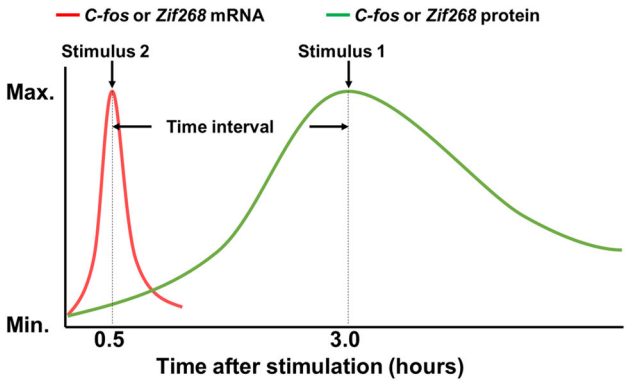

Fig. 1 Principle of dual-epoch mapping techniques such as I-FISH and TAI-FISH. These methods use *Zif268* or *c-fos* mRNA and protein signals to differentially label neural ensembles induced by two different stimuli. In TAI-FISH, Xiu *et al.* [19, 20] used tyramide to improve the signal-to-noise ratio of IHC and achieved better temporal separation between *c-fos* mRNA and protein signals than I-FISH.

Chaudhuri *et al.* first developed a technique using regular IHC and fluorescent ISH (abbreviated as I-FISH) to detect *Zif268* signals to label and differentiate neurons activated by different sensory stimuli [17, 18]. Inspired by this technique, Xiu *et al.* developed tyramide-amplified IHC–FISH (TAI-FISH) to further investigate neural activations in the prelimbic system stimulated by either appetitive or aversive stimuli [19, 20]. In TAI-FISH, tyramide was used to further amplify IHC signals to improve the signal-to-noise ratio and more robustly separate the protein and mRNA signal peaks induced by two stimuli. Using *c-fos*-based TAI-FISH, Xiu and colleagues found that appetitive and aversive valences are coded by largely distinct, often spatially separated neural ensembles in many of the same brain regions, thus indicating that different emotional valences are coded by distinct neural circuits.

Imaging Neural Projections Using IEG-Dependent Signals at the Whole-Brain Scale

In addition to visualizing activated neuronal cell bodies, mapping of their projections across the whole brain is also required to enable systemic identification of brain circuits that are functionally involved in different behaviors, and to assess whether and how they are functionally connected. But aside from several hundred micrometers of cortical layers, the deep brain is impenetrable to the light microscope. Meanwhile, conventional brain sectioning

techniques lack the necessary resolution for reconstructing projections that constitute a neural network.

Two different strategies have been developed to solve this problem. Optical sectioning technologies, which include BBAB [21], ScaleA2 [22], 3DISCO [23, 24], ClearT2 [25], SeeDB [26], CLARITY [10, 27, 28], CUBIC [29], iDISCO [30, 31], and PACT [32], use special solutions to clear brain tissues by dissolving lipids while preserving the rest of the structure, most importantly neurons and projections, thus matching the refractive indexes between brain regions and reducing light scatter so that neurons and projections once hidden deep in the brain can now be imaged [33].

Alternatively, fluorescent Micro-Optical Sectioning Tomography (fMOST) combines ultrathin mechanical sectioning, simultaneous imaging, and 3D-image reconstruction to scan the whole mouse brain to image fluorescent protein-labeled neurons and their projections at micron-scale resolution [34–36]. This was further improved by chemically reactivating fluorescent protein signals after sample embedding [37]. Thus, fMOST is compatible with the IEG-dependent tools that express fluorescent proteins to label activated neural networks.

So far, CLARITY has been used to map *c-fos*-driven tdTomato signals induced by cocaine or foot shock [10]. All of these techniques are compatible with fluorescent protein visualization, and thus can be used in conjunction with IEG-dependent labeling tools (see next section). It will be exciting to see what new neural ensembles and functional circuits will be revealed with these imaging technologies.

IEG-Dependent Molecular Tools to Functionally Label and Manipulate Activated Neural Ensembles

Complementing endogenous-IEG-based methods, in the last two decades, a variety of IEG-dependent molecular tools, either in the form of transgenic animals or virus-based expression constructs, have been developed to study neural activation [38].

Some of these tools use IEG promoters to activate the expression of a reporter to label activated neurons. The most frequently-used reporter is a fluorescent protein [39–45], although beta-galactosidase (*lacZ*) [46] and luciferase [47, 48] have also been used. In addition to regular fluorescent proteins, new species like d2EGFP that has a shorter half-life, or "fluorescent timers" which change color over time after being translated [49], have also been used to either reduce the non-specific labeling caused by leaky expression [44, 50–52], or to differentially label neurons activated at different time points [53].

Some of these tools express effector genes to manipulate the activated ensembles. For example, *cfos-LacZ* has also been used to convert the infused compound Daun02 to daunorubicin to inhibit Ca^{2+}-dependent neuronal activity. This technique has been used to identify and manipulate neurons involved in contextual drug conditioning and food-seeking behaviors [46, 54–57], although it should be noted that the robustness and specificity of the *LacZ*-Daun02 technique has yet to be fully quantified and hence evaluated as illustrated in Fig. 2 and the section entitled "Evaluation of the Robustness and Specificity of IEG-Dependent Tools".

Today, opsins such as channel rhodopsin [58, 59], halorhodopsin [60], and archaerhodopsin [61] are the most frequently used effectors and have been shown to be able to bidirectionally manipulate neural ensembles involved in memory formation [53, 62–65], innate and learned behaviors [66, 67], and contextual fear conditioning [64, 65]. DREADD (designer receptor exclusively activated by designer drug) receptors [68, 69] have also been used to activate or inhibit stimulated ensembles [70].

To ensure that the reporters and effectors are both exclusively and robustly expressed in stimuli-activated neurons and nowhere else, both native IEG promoters such as *c-fos*, *Arc*, and *Egr1* [44, 67, 71, 72], and native enhancers such as the Synaptic Activity-Responsive Element (SARE) of the *Arc* gene (used in conjunction with a minimal *Arc* promoter) have been successfully used to label and manipulate activated neurons and spines [52, 73]. Furthermore, synthetic promoters have been designed to combine multiple discrete regulatory motifs with minimal IEG promoters to express the reporter or effector genes more robustly, or to reduce background neural labeling. For example, the Robust Activity Marking system fuses the Activator Protein-1 site and *Npas4*-Responsive Element sites to a minimal human *FOS* promoter to induce >30-fold induction of labeling after contextual fear conditioning in the hippocampal CA3 region [74]. Similarly, the enhanced SARE system clustered multiple subregions of the native SARE enhancer to a minimal *Arc* promoter, and it demonstrated far stronger inducibility in labeling contralateral V1 layer 2/3 neurons in a monocular stimulation paradigm than a *cfos* promoter [50].

"Two-Tiered" IEG-Dependent Tools and Their Temporal Control Mechanisms

One major challenge for the IEG-dependent molecular tools is to minimize the activity of IEG promoters in the absence of a stimulus, because leaky activity of the IEG-dependent promoter may cause substantial background neuron labeling or effector expression. To solve this

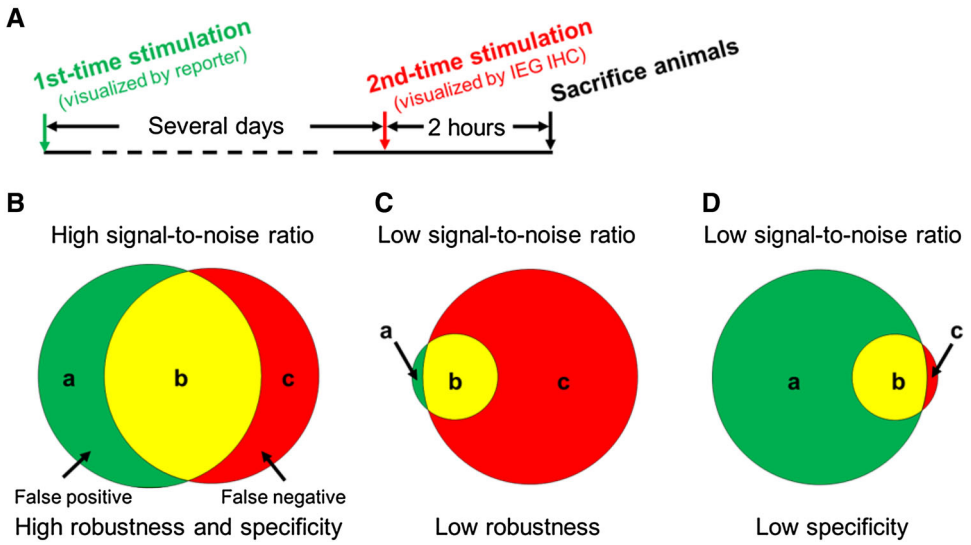

Fig. 2 Experimental procedure to quantify the robustness and specificity of IEG-dependent tools. **A** Two identical stimuli are applied several days apart (based on the literature [66, 85, 88] and our own tests, the exact time interval between the two stimuli may depend on the tools, brain regions, and behavioral paradigms used) to induce signals in the IEG-dependent tool and endogenous IEG, respectively. **B** Signals of an IEG-dependent tool are divided into two parts: false positives (neurons only labeled by the IEG-dependent tool, a); and true positives (neurons labeled by both the IEG-dependent tool and endogenous IEG staining, b). The third category, false negative signals (c) are neurons only labeled by endogenous IEG staining. We quantify the robustness of an IEG-dependent tool as b/(b+c), and its specificity by b/(a+b). Examples of low robustness (**C**) and low specificity (**D**) are shown. A given IEG-dependent tool needs to have both high robustness and specificity to have a high signal-to-noise ratio.

problem, "two-tiered" IEG-dependent tools have been developed in recent years.

In these tools, an IEG promoter drives the expression of a primary effector gene (the first tier) when being stimulated by the intended stimulus (foot shocks, for example). The primary effector itself does not label or manipulate activated neurons. Instead, it activates the expression of a secondary reporter or effector gene (the second tier) for the actual labeling or manipulation.

The key feature of a two-tiered IEG-dependent tool is that an additional layer of temporal control is incorporated to minimize the activity of the primary effector gene in the absence of the intended stimulus, hence the expression of the second-tier reporter or effector in neurons is also minimized. Only when the intended stimulus is to be given is the temporal control mechanism removed to allow the expression of the second-tier genes.

The TetTag mouse is one such tool that has been extensively used to tag and manipulate neurons involved in memory formation in the hippocampus, basolateral amygdala, and medial prefrontal cortex [62–65, 70, 75–77]. The TetTag transgenic mouse line uses the Tet-Off system to turn off the expression of a reporter or effector in the absence of the intended stimulus [76, 78] (Fig. 3A). In the TetTag mouse, the primary effector is tetracycline transactivator (tTA), an artificial transcription activator. Accordingly, the "second tier" gene has a synthetic promoter which contains tetracycline response elements (TREs) and requires tTA to bind the TREs for expression.

Prior to stimulation, TetTag mice are fed a diet containing doxycycline (Dox), which binds to the cellular tTA and prevents it from binding TREs, thus preventing the reporter or effector gene from being expressed. Several days before stimulation, the TetTag mouse is switched to a diet without Dox for clearance. This provides a time window for stimulation, and for stimulus-induced tTA to bind TREs and activate the expression of the secondary reporter or effector. After stimulation, the TetTag mouse is switched back to a Dox-containing diet again to minimize tTA activity. In doing so the expression of the second tier reporter and effector gene is strictly limited to the period when the intended stimulus is given.

Another two-tiered system uses creER as the primary effector gene (Fig. 3B). creER is a derivative of cre recombinase, fused with a mutated ligand-binding domain for the human estrogen receptor (ER) [79–81]. The ER domain prevents creER from entering the nucleus without tamoxifen, an ER antagonist. The secondary reporter or effector gene is either constructed as a double-floxed inverse open reading frame (DIO or FLEX) [82], thus is in the opposite direction to its own promoter, or is prevented from being translated by a loxp-stop-loxp sequence which is placed between the effectors and their promoters [83, 84]. Therefore, in the absence of tamoxifen, cellular

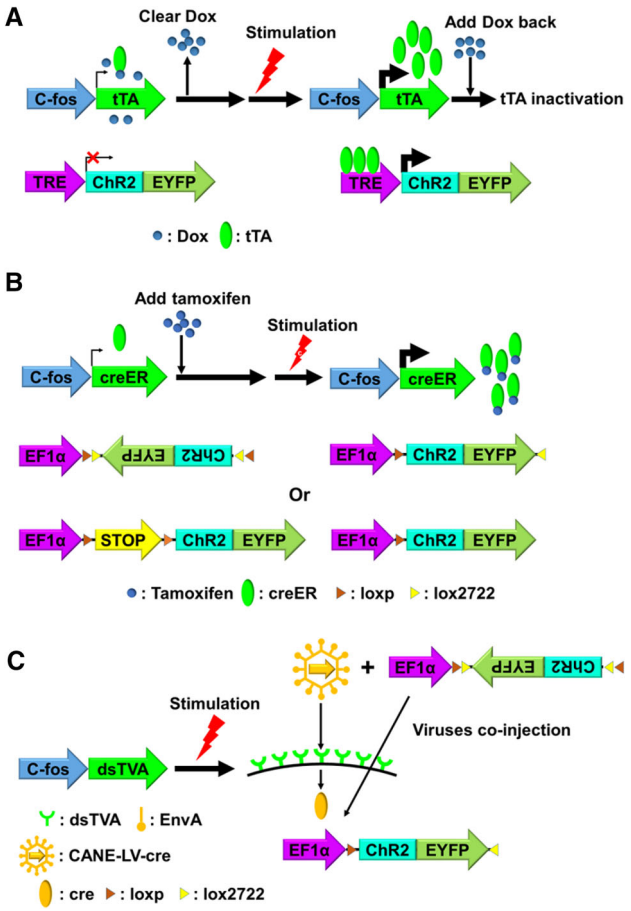

Fig. 3 Three "two-tiered" IEG-dependent tools (**A**: Tet-OFF; **B**: creER; **C**: CANE) and their respective mechanisms for temporal control. ChR2-EYFP is the reporter-effector for all three tools [64, 67, 88]. In CANE (**C**), AAV-DIO-ChR2-EYFP is co-injected with CANE-LV-cre.

creER is kept in the cytoplasm and prevented from entering the nucleus, and is unable to reorganize the expression construct of the secondary reporter or effector to allow its expression.

For stimulation, typically, animals are injected a few hours ahead with tamoxifen, which binds to the ER domain and allows stimulus-induced creER to enter the nucleus, where it either "flips" the secondary reporter or effector gene to allow transcription [67, 85, 86], or removes the intervening loxp-stop-loxp sequence to allow translation [87]. Using this strategy, *Arc*-CreER and TRAP transgenic mice have been generated to investigate neural ensembles activated by innate or learned responses, complex experiences, and an appetitive or aversive emotional stimulus [10, 67, 85, 87].

A more recent "two-tiered" system is called CANE (capturing activated neuronal ensembles) [88] (Fig. 3C). In the CANE system, the primary effector gene is a destabilized version of TVA (dsTVA), an avian membrane receptor, which is inserted to the cell membrane of activated neurons. The secondary reporter or effector is delivered by pseudo-viral vehicles coated with EnvA, a ligand of TVA. This ensures precise targeting of the secondary reporter or effector to the stimulated, TVA-expressing neurons for expression.

Because of its short half-life, the level of dsTVA prior to stimulation is very low. Indeed, the secondary reporter or effector must be delivered to activated neurons within one to two hours after stimulation. This relatively narrow time window for targeting provides much tighter temporal control over expressing the reporter or effector genes in activated neurons than other systems, and thus more effectively minimizes non-specific expression.

IEG-Based Methods to Analyze the Molecular Features of Neural Ensembles

IEG-dependent molecular tools are also suitable for revealing the gene expression profiles of neural ensembles activated by behavior or experience. By tagging ribosomes or mRNA of activated neurons and then using immunoprecipitation (IP) to isolate translating mRNA for analysis, two groups have identified the molecular signatures of emotion-related ensembles in the medial prefrontal cortex [10] and basolateral amygdala [13]. In addition to using IEG-dependent molecular tools, it is now technically feasible to isolate activated neural ensembles for transcriptome profiling using IEG markers [89–91] or phosphorylated ribosomes [92]. By analyzing the transcriptional landscapes of activated neural ensembles, we may discover new sets of genes whose expression is significantly and rapidly altered by a given stimulus.

Evaluation of the Robustness and Specificity of IEG-Dependent Tools

IEG-dependent molecular tools have been developed to simplify the identification of stimuli-activated neural ensembles, and arguably more importantly, to install effectors such as opsin in such ensembles for future manipulation. Therefore, they need to capture neurons that are genuinely activated by the stimulus. As such, endogenous IEG activation patterns are the gold standards to evaluate a given IEG-dependent tool, which ideally should label an identical or a very similar activated neural ensemble as the endogenous IEG in response to the same stimulus.

We and others have used the experimental procedures illustrated in Fig. 2A to quantify the signal-to-noise ratio of IEG-dependent tools [66, 85, 88]. Specifically, we use two parameters to evaluate an IEG-dependent tool: first,

robustness/penetrance, which we define as the percentage of neurons labeled by endogenous IEG signals that are also labeled by the IEG-dependent reporter (b/b+c in Fig. 2B); and second, specificity/faithfulness, defined by the percentage of neurons labeled by the IEG-dependent reporter that are also labeled by endogenous IEG signals (b/a+b in Fig. 2B). A low degree of robustness causes insufficient labeling or installation of effectors into activated neurons (false negatives, Fig. 2C). Low specificity leads to the labeling and manipulation of neurons that are not activated by stimulation (false positives, Fig. 2D). Both cause less desirable signal-to-noise ratios, and thus should be avoided.

Some factors are known to affect the signal-to-noise ratio of specific IEG-dependent tools. For example, IEG-tTA and IEG-creER are significantly influenced by the metabolic rate of Dox and tamoxifen, respectively: Dox clearance takes days to weeks to be effective so residual Dox no longer blocks tTA from inducing the robust transcription of the secondary reporter or effector [76, 97]; similarly, tamoxifen takes several hours to induce sufficient creER entry into the nucleus [85]. If a stimulus is given too early, i.e. before Dox or tamoxifen reaches its optimal concentration, it could cause insufficient expression of the reporter or effector; alternatively, if a stimulus is given too late, the basal level of tTA or creER may cause substantial expression of reporter or effector genes in neurons activated by unintended stimuli. Therefore, researchers using these tools need to carefully optimize the time windows of Dox clearance or tamoxifen induction to ensure the optimal signal-to-noise ratio.

Furthermore, based on previous publications and our own tests [66, 85, 88], the signal-to-noise ratio of IEG-dependent tools can vary significantly between different brain regions or behavioral paradigms (unpublished data): they may be robustly activated by stimuli in some brain regions and have neural activation patterns similar to endogenous IEGs, but have poor signal-to-noise ratios in other brain regions and/or behavioral paradigms. Therefore, researchers should thoroughly test their IEG-dependent tools of choice to determine whether they have satisfactory signal-to-noise ratios for the brain regions and/or behaviors of interest (Fig. 2).

Limitations of IEG-Dependent Tools

No tools are perfect. IEG-based molecular tools do have limitations: first, there is likely a threshold of electrophysiological activity that must be passed before a neuron expresses IEG (e.g. bursting activity), so IEG mapping only reveals a subset of those neurons that actively contribute to a behavior; second, some brain areas can show strong electrophysiological activation without expressing IEGs, e.g. the substantia nigra does not express c-fos despite robust activity [98–100]; and third, the basal levels of IEG genes can be high in some brain areas (e.g. sensory and motor cortices) [19, 20, 101, 102], thus preventing specific labeling. In these regards, other methods such as functional magnetic resonance imaging [103] and single-unit recording [11, 104, 105] can provide complementary information.

Non-IEG-Based Activity-Dependent Tools

Last year, a new class of activity-dependent tools was introduced: the Ca^{2+}-and-light-gated tools, which include Cal-Light [93] and FLARE [94]. Unlike the tools described above, these do not use IEG sequences. Instead, they are designed to label and install effectors in activated neurons in response to the rise of cytoplasmic Ca^{2+} after neuronal activation. In addition, photostimulation is incorporated to provide temporal and spatial control to minimize non-specific expression of the reporter or effector gene.

Cal-Light and FLARE both express two multi-domain fusion proteins. One fusion protein contains five domains: the transcription factor tTA, which drives the expression of reporter and effector genes in the activated neurons; a transmembrane domain, which tethers tTA to the cell surface; a light-oxygen-voltage (LOV) [95] sensing domain for light gating; a Ca^{2+}-gating domain (calmodulin (CaM) or CaM-binding peptide); and the tobacco etch virus protease (TEVp) cleavage sequence (TEVseq) to release tethered tTA[96].

The other fusion protein contains two main domains: another Ca^{2+}-gating domain that mediates the interaction between the two fusion proteins in the presence of high cytoplasmic Ca^{2+}; and TEVp, which cleaves the TEVseq to release tTA. A third construct in these tools carries the reporter and effector genes controlled by a TRE sequence recognized by tTA.

In stimulated neurons, an influx of Ca^{2+} triggers a robust interaction between the two Ca^{2+}-gating domains, which brings TEVp into close proximity with TEVseq. However, the LOV domain blocks TEVseq from being accessed by TEVp, so an undesired rise of Ca^{2+} alone is insufficient to induce TEVp cleavage and tTA release. After minutes of blue-light exposure, LOV undergoes conformational changes and exposes TEVseq to TEVp for TEVp cleavage, tTA release, and the expression of reporter and effector genes in the activated neurons.

Like the two-tiered IEG-dependent tools described earlier, the Cal-Light and FLARE tools are capable of converting transient neural activation patterns into stable neural labeling and effector installation *via* transcriptional activation, which offers significant versatility in

choosing reporters and effectors. Most importantly, they provide tighter spatiotemporal control, especially due to the much narrower time window and smaller area of light exposure than in previous IEG-dependent tools. On the other hand, since Cal-Light and FLARE require the co-transfection of three viral constructs into the same neuron, and the ratio between the two fusion proteins affects the level of tTA release [93], additional tests may be required to determine the appropriate dosage of each construct for an application. Nevertheless, it will be exciting to see the further optimization and application of these new tools.

Acknowledgements This review was supported by the National Natural Science Foundation of China (81571335, 91432108 and 81527901) and grants from the Ministry of Science and Technology of China (2016YFA0501000).

Compliance with Ethical Standards

Conflict of interest All authors claim that there are no conflicts of interest.

References

1. Anderson DJ, Adolphs R. A framework for studying emotions across species. Cell 2014, 157: 187–200.
2. Hu H. Reward and aversion. Annu Rev Neurosci 2016, 39: 297–324.
3. Cole AJ, Saffen DW, Baraban JM, Worley PF. Rapid increase of an immediate early gene messenger RNA in hippocampal neurons by synaptic NMDA receptor activation. Nature 1989, 340: 474–476.
4. Bartel DP, Sheng M, Lau LF, Greenberg ME. Growth factors and membrane depolarization activate distinct programs of early response gene expression: dissociation of fos and jun induction. Genes Dev 1989, 3: 304–313.
5. Morgan JI, Cohen DR, Hempstead JL, Curran T. Mapping patterns of c-fos expression in the central nervous system after seizure. Science 1987, 237: 192–197.
6. Moratalla R, Robertson HA, Graybiel AM. Dynamic regulation of NGFI-A (zif268, egr1) gene expression in the striatum. J Neurosci 1992, 12: 2609–2622.
7. Hope B, Kosofsky B, Hyman SE, Nestler EJ. Regulation of immediate early gene expression and AP-1 binding in the rat nucleus accumbens by chronic cocaine. Proc Natl Acad Sci U S A 1992, 89: 5764–5768.
8. Johnson ZV, Revis AA, Burdick MA, Rhodes JS. A similar pattern of neuronal Fos activation in 10 brain regions following exposure to reward- or aversion-associated contextual cues in mice. Physiol Behav 2010, 99: 412–418.
9. Lammel S, Lim BK, Ran C, Huang KW, Betley MJ, Tye KM, *et al.* Input-specific control of reward and aversion in the ventral tegmental area. Nature 2012, 491: 212–217.
10. Ye L, Allen WE, Thompson KR, Tian Q, Hsueh B, Ramakrishnan C, *et al.* Wiring and molecular features of prefrontal ensembles representing distinct experiences. Cell 2016, 165: 1776–1788.
11. Beyeler A, Namburi P, Glober GF, Simonnet C, Calhoon GG, Conyers GF, *et al.* Divergent routing of positive and negative information from the amygdala during memory retrieval. Neuron 2016, 90: 348–361.
12. Namburi P, Beyeler A, Yorozu S, Calhoon GG, Halbert SA, Wichmann R, *et al.* A circuit mechanism for differentiating positive and negative associations. Nature 2015, 520: 675–678.
13. Kim J, Pignatelli M, Xu S, Itohara S, Tonegawa S. Antagonistic negative and positive neurons of the basolateral amygdala. Nat Neurosci 2016, 19: 1636–1646.
14. Guzowski JF, Setlow B, Wagner EK, McGaugh JL. Experience-dependent gene expression in the rat hippocampus after spatial learning: a comparison of the immediate-early genes Arc, c-fos, and zif268. J Neurosci 2001, 21: 5089–5098.
15. Guzowski JF, Worley PF. Cellular compartment analysis of temporal activity by fluorescence in situ hybridization (cat-FISH). Curr Protoc Neurosci 2001, 15: 1–8.
16. Lin D, Boyle MP, Dollar P, Lee H, Lein ES, Perona P, *et al.* Functional identification of an aggression locus in the mouse hypothalamus. Nature 2011, 470: 221–226.
17. Chaudhuri A, Nissanov J, Larocque S, Rioux L. Dual activity maps in primate visual cortex produced by different temporal patterns of zif268 mRNA and protein expression. Proc Natl Acad Sci U S A 1997, 94: 2671–2675.
18. Zangenehpour S, Chaudhuri A. Neural activity profiles of the neocortex and superior colliculus after bimodal sensory stimulation. Cereb Cortex 2001, 11: 924–935.
19. Xiu J, Zhang Q, Zhou T, Zhou TT, Chen Y, Hu H. Visualizing an emotional valence map in the limbic forebrain by TAI–FISH. Nat Neurosci 2014, 17: 1552–1559.
20. Zhang Q, He Q, Wang J, Fu C, Hu H. Use of TAI-FISH to visualize neural ensembles activated by multiple stimuli. Nat Protoc 2018, 13: 118–133.
21. Becker K, Jahrling N, Saghafi S, Weiler R, Dodt HU. Chemical clearing and dehydration of GFP expressing mouse brains. PLoS One 2012, 7: e33916.
22. Hama H, Kurokawa H, Kawano H, Ando R, Shimogori T, Noda H, *et al.* Scale: a chemical approach for fluorescence imaging and reconstruction of transparent mouse brain. Nat Neurosci 2011, 14: 1481–1488.
23. Erturk A, Becker K, Jahrling N, Mauch CP, Hojer CD, Egen JG, *et al.* Three-dimensional imaging of solvent-cleared organs using 3DISCO. Nat Protoc 2012, 7: 1983–1995.
24. Erturk A, Mauch CP, Hellal F, Forstner F, Keck T, Becker K, *et al.* Three-dimensional imaging of the unsectioned adult spinal cord to assess axon regeneration and glial responses after injury. Nat Med 2011, 18: 166–171.
25. Kuwajima T, Sitko AA, Bhansali P, Jurgens C, Guido W, Mason C. ClearT: a detergent- and solvent-free clearing method for neuronal and non-neuronal tissue. Development 2013, 140: 1364–1368.
26. Ke MT, Fujimoto S, Imai T. SeeDB: a simple and morphology-preserving optical clearing agent for neuronal circuit reconstruction. Nat Neurosci 2013, 16: 1154–1161.
27. Tomer R, Ye L, Hsueh B, Deisseroth K. Advanced CLARITY for rapid and high-resolution imaging of intact tissues. Nat Protoc 2014, 9: 1682–1697.
28. Chung K, Wallace J, Kim SY, Kalyanasundaram S, Andalman AS, Davidson TJ, *et al.* Structural and molecular interrogation of intact biological systems. Nature 2013, 497: 332–337.
29. Susaki EA, Tainaka K, Perrin D, Kishino F, Tawara T, Watanabe TM, *et al.* Whole-brain imaging with single-cell resolution using chemical cocktails and computational analysis. Cell 2014, 157: 726–739.
30. Renier N, Wu Z, Simon DJ, Yang J, Ariel P, Tessier-Lavigne M. iDISCO: a simple, rapid method to immunolabel large tissue samples for volume imaging. Cell 2014, 159: 896–910.
31. Renier N, Adams EL, Kirst C, Wu Z, Azevedo R, Kohl J, *et al.* Mapping of brain activity by automated volume analysis of immediate early genes. Cell 2016, 165: 1789–1802.

32. Yang B, Treweek JB, Kulkarni RP, Deverman BE, Chen CK, Lubeck E, *et al.* Single-cell phenotyping within transparent intact tissue through whole-body clearing. Cell 2014, 158: 945–958.
33. Theer P, Denk W. On the fundamental imaging-depth limit in two-photon microscopy. J Opt Soc Am A Opt Image Sci Vis 2006, 23: 3139–3149.
34. Li A, Gong H, Zhang B, Wang Q, Yan C, Wu J, *et al.* Micro-optical sectioning tomography to obtain a high-resolution atlas of the mouse brain. Science 2010, 330: 1404–1408.
35. Zheng T, Yang Z, Li A, Lv X, Zhou Z, Wang X, *et al.* Visualization of brain circuits using two-photon fluorescence micro-optical sectioning tomography. Opt Express 2013, 21: 9839–9850.
36. Gong H, Zeng S, Yan C, Lv X, Yang Z, Xu T, *et al.* Continuously tracing brain-wide long-distance axonal projections in mice at a one-micron voxel resolution. Neuroimage 2013, 74: 87–98.
37. Xiong H, Zhou Z, Zhu M, Lv X, Li A, Li S, *et al.* Chemical reactivation of quenched fluorescent protein molecules enables resin-embedded fluorescence microimaging. Nat Commun 2014, 5: 3992.
38. Gore F, Schwartz EC, Salzman CD. Manipulating neural activity in physiologically classified neurons: triumphs and challenges. Philos Trans R Soc Lond B Biol Sci 2015, 370: 20140216.
39. Kasof GM, Mandelzys A, Maika SD, Hammer RE, Curran T, Morgan JI. Kainic acid-induced neuronal death is associated with DNA damage and a unique immediate-early gene response in c-fos-lacZ transgenic rats. J Neurosci 1995, 15: 4238–4249.
40. Wilson Y, Nag N, Davern P, Oldfield BJ, McKinley MJ, Greferath U, *et al.* Visualization of functionally activated circuitry in the brain. Proc Natl Acad Sci U S A 2002, 99: 3252–3257.
41. Barth AL, Gerkin RC, Dean KL. Alteration of neuronal firing properties after *in vivo* experience in a FosGFP transgenic mouse. J Neurosci 2004, 24: 6466–6475.
42. Knapska E, Macias M, Mikosz M, Nowak A, Owczarek D, Wawrzyniak M, *et al.* Functional anatomy of neural circuits regulating fear and extinction. Proc Natl Acad Sci U S A 2012, 109: 17093–17098.
43. Mikuni T, Uesaka N, Okuno H, Hirai H, Deisseroth K, Bito H, *et al.* Arc/Arg3.1 is a postsynaptic mediator of activity-dependent synapse elimination in the developing cerebellum. Neuron 2013, 78: 1024–1035.
44. Wang KH, Majewska A, Schummers J, Farley B, Hu C, Sur M, *et al. In vivo* two-photon imaging reveals a role of arc in enhancing orientation specificity in visual cortex. Cell 2006, 126: 389–402.
45. Kim Y, Perova Z, Mirrione MM, Pradhan K, Henn FA, Shea S, *et al.* Whole-brain mapping of neuronal activity in the learned helplessness model of depression. Front Neural Circuits 2016, 10: 3.
46. Koya E, Golden SA, Harvey BK, Guez-Barber DH, Berkow A, Simmons DE, *et al.* Targeted disruption of cocaine-activated nucleus accumbens neurons prevents context-specific sensitization. Nat Neurosci 2009, 12: 1069–1073.
47. Boer U, Alejel T, Beimesche S, Cierny I, Krause D, Knepel W, *et al.* CRE/CREB-driven up-regulation of gene expression by chronic social stress in CRE-luciferase transgenic mice: reversal by antidepressant treatment. PLoS One 2007, 2: e431.
48. Geusz ME, Fletcher C, Block GD, Straume M, Copeland NG, Jenkins NA, *et al.* Long-term monitoring of circadian rhythms in c-fos gene expression from suprachiasmatic nucleus cultures. Curr Biol 1997, 7: 758–766.
49. Subach FV, Subach OM, Gundorov IS, Morozova KS, Piatkevich KD, Cuervo AM, *et al.* Monomeric fluorescent timers that change color from blue to red report on cellular trafficking. Nat Chem Biol 2009, 5: 118–126.
50. Kawashima T, Kitamura K, Suzuki K, Nonaka M, Kamijo S, Takemoto-Kimura S, *et al.* Functional labeling of neurons and their projections using the synthetic activity-dependent promoter E-SARE. Nat Methods 2013, 10: 889–895.
51. Eguchi M, Yamaguchi S. *In vivo* and *in vitro* visualization of gene expression dynamics over extensive areas of the brain. Neuroimage 2009, 44: 1274–1283.
52. Kawashima T, Okuno H, Nonaka M, Adachi-Morishima A, Kyo N, Okamura M, *et al.* Synaptic activity-responsive element in the Arc/Arg3.1 promoter essential for synapse-to-nucleus signaling in activated neurons. Proc Natl Acad Sci U S A 2009, 106: 316–321.
53. Okuyama T, Kitamura T, Roy DS, Itohara S, Tonegawa S. Ventral CA1 neurons store social memory. Science 2016, 353: 1536–1541.
54. Cruz FC, Babin KR, Leao RM, Goldart EM, Bossert JM, Shaham Y, *et al.* Role of nucleus accumbens shell neuronal ensembles in context-induced reinstatement of cocaine-seeking. J Neurosci 2014, 34: 7437–7446.
55. Bossert JM, Stern AL, Theberge FR, Cifani C, Koya E, Hope BT, *et al.* Ventral medial prefrontal cortex neuronal ensembles mediate context-induced relapse to heroin. Nat Neurosci 2011, 14: 420–422.
56. Xue YX, Chen YY, Zhang LB, Zhang LQ, Huang GD, Sun SC, *et al.* Selective inhibition of amygdala neuronal ensembles encoding nicotine-associated memories inhibits nicotine preference and relapse. Biol Psychiatry 2017, 82: 781–793. .
57. Warren BL, Mendoza MP, Cruz FC, Leao RM, Caprioli D, Rubio FJ, *et al.* Distinct Fos-expressing neuronal ensembles in the ventromedial prefrontal cortex mediate food reward and extinction memories. J Neurosci 2016, 36: 6691–6703.
58. Boyden ES, Zhang F, Bamberg E, Nagel G, Deisseroth K. Millisecond-timescale, genetically targeted optical control of neural activity. Nat Neurosci 2005, 8: 1263-1268.
59. Zhang F, Wang LP, Boyden ES, Deisseroth K. Channelrhodopsin-2 and optical control of excitable cells. Nat Methods 2006, 3: 785–792.
60. Zhao S, Cunha C, Zhang F, Liu Q, Gloss B, Deisseroth K, *et al.* Improved expression of halorhodopsin for light-induced silencing of neuronal activity. Brain Cell Biol 2008, 36: 141–154.
61. Han X, Chow BY, Zhou H, Klapoetke NC, Chuong A, Rajimehr R, *et al.* A high-light sensitivity optical neural silencer: development and application to optogenetic control of non-human primate cortex. Front Syst Neurosci 2011, 5: 18.
62. Redondo RL, Kim J, Arons AL, Ramirez S, Liu X, Tonegawa S. Bidirectional switch of the valence associated with a hippocampal contextual memory engram. Nature 2014, 513: 426–430.
63. Ramirez S, Liu X, MacDonald CJ, Moffa A, Zhou J, Redondo RL, *et al.* Activating positive memory engrams suppresses depression–like behaviour. Nature 2015, 522: 335–339.
64. Liu X, Ramirez S, Pang PT, Puryear CB, Govindarajan A, Deisseroth K, *et al.* Optogenetic stimulation of a hippocampal engram activates fear memory recall. Nature 2012, 484: 381–385.
65. Ramirez S, Liu X, Lin PA, Suh J, Pignatelli M, Redondo RL, *et al.* Creating a false memory in the hippocampus. Science 2013, 341: 387–391.
66. Gore F, Schwartz EC, Brangers BC, Aladi S, Stujenske JM, Likhtik E, *et al.* Neural representations of unconditioned stimuli in basolateral amygdala mediate innate and learned responses. Cell 2015, 162: 134–145.

67. Root CM, Denny CA, Hen R, Axel R. The participation of cortical amygdala in innate, odour-driven behaviour. Nature 2014, 515: 269–273.
68. Armbruster BN, Li X, Pausch MH, Herlitze S, Roth BL. Evolving the lock to fit the key to create a family of G protein-coupled receptors potently activated by an inert ligand. Proc Natl Acad Sci U S A 2007, 104: 5163–5168.
69. Dong S, Rogan SC, Roth BL. Directed molecular evolution of DREADDs: a generic approach to creating next-generation RASSLs. Nat Protoc 2010, 5: 561–573.
70. Garner AR, Rowland DC, Hwang SY, Baumgaertel K, Roth BL, Kentros C, *et al.* Generation of a synthetic memory trace. Science 2012, 335: 1513–1516.
71. Man PS, Wells T, Carter DA. Egr-1-d2EGFP transgenic rats identify transient populations of neurons and glial cells during postnatal brain development. Gene Expr Patterns 2007, 7: 872–883.
72. Xie H, Liu Y, Zhu Y, Ding X, Yang Y, Guan JS. *In vivo* imaging of immediate early gene expression reveals layer-specific memory traces in the mammalian brain. Proc Natl Acad Sci U S A 2014, 111: 2788–2793.
73. Hayashi-Takagi A, Yagishita S, Nakamura M, Shirai F, Wu YI, Loshbaugh AL, *et al.* Labelling and optical erasure of synaptic memory traces in the motor cortex. Nature 2015, 525: 333–338.
74. Sorensen AT, Cooper YA, Baratta MV, Weng FJ, Zhang Y, Ramamoorthi K, *et al.* A robust activity marking system for exploring active neuronal ensembles. Elife 2016, 5: e13918.
75. Matsuo N, Reijmers L, Mayford M. Spine-type-specific recruitment of newly synthesized AMPA receptors with learning. Science 2008, 319: 1104–1107.
76. Reijmers LG, Perkins BL, Matsuo N, Mayford M. Localization of a stable neural correlate of associative memory. Science 2007, 317: 1230–1233.
77. Kitamura T, Ogawa SK, Roy DS, Okuyama T, Morrissey MD, Smith LM, *et al.* Engrams and circuits crucial for systems consolidation of a memory. Science 2017, 356: 73–78.
78. Gossen M, Bujard H. Tight control of gene expression in mammalian cells by tetracycline-responsive promoters. Proc Natl Acad Sci U S A 1992, 89: 5547–5551.
79. Feil R, Brocard J, Mascrez B, LeMeur M, Metzger D, Chambon P. Ligand-activated site-specific recombination in mice. Proc Natl Acad Sci U S A 1996, 93: 10887–10890.
80. Metzger D, Clifford J, Chiba H, Chambon P. Conditional site-specific recombination in mammalian cells using a ligand-dependent chimeric Cre recombinase. Proc Natl Acad Sci U S A 1995, 92: 6991–6995.
81. Feil R, Wagner J, Metzger D, Chambon P. Regulation of Cre recombinase activity by mutated estrogen receptor ligand-binding domains. Biochem Biophys Res Commun 1997, 237: 752–757.
82. Sohal VS, Zhang F, Yizhar O, Deisseroth K. Parvalbumin neurons and gamma rhythms enhance cortical circuit performance. Nature 2009, 459: 698–702.
83. Madisen L, Mao T, Koch H, Zhuo JM, Berenyi A, Fujisawa S, *et al.* A toolbox of Cre-dependent optogenetic transgenic mice for light-induced activation and silencing. Nat Neurosci 2012, 15: 793–802.
84. Madisen L, Zwingman TA, Sunkin SM, Oh SW, Zariwala HA, Gu H, *et al.* A robust and high-throughput Cre reporting and characterization system for the whole mouse brain. Nat Neurosci 2010, 13: 133–140.
85. Guenthner CJ, Miyamichi K, Yang HH, Heller HC, Luo L. Permanent genetic access to transiently active neurons via TRAP: targeted recombination in active populations. Neuron 2013, 78: 773–784.
86. Allen WE, DeNardo LA, Chen MZ, Liu CD, Loh KM, Fenno LE, *et al.* Thirst-associated preoptic neurons encode an aversive motivational drive. Science 2017, 357: 1149–1155.
87. Denny CA, Kheirbek MA, Alba EL, Tanaka KF, Brachman RA, Laughman KB, *et al.* Hippocampal memory traces are differentially modulated by experience, time, and adult neurogenesis. Neuron 2014, 83: 189–201.
88. Sakurai K, Zhao S, Takatoh J, Rodriguez E, Lu J, Leavitt AD, *et al.* Capturing and manipulating activated neuronal ensembles with CANE delineates a hypothalamic social-fear circuit. Neuron 2016, 92: 739–753.
89. Heiman M, Schaefer A, Gong S, Peterson JD, Day M, Ramsey KE, *et al.* A translational profiling approach for the molecular characterization of CNS cell types. Cell 2008, 135: 738–748.
90. Li K, Nakajima M, Ibanez-Tallon I, Heintz N. A cortical circuit for sexually dimorphic oxytocin-dependent anxiety behaviors. Cell 2016, 167: 60–72 e11.
91. Guez-Barber D, Fanous S, Golden SA, Schrama R, Koya E, Stern AL, *et al.* FACS identifies unique cocaine-induced gene regulation in selectively activated adult striatal neurons. J Neurosci 2011, 31: 4251–4259.
92. Knight ZA, Tan K, Birsoy K, Schmidt S, Garrison JL, Wysocki RW, *et al.* Molecular profiling of activated neurons by phosphorylated ribosome capture. Cell 2012, 151: 1126–1137.
93. Lee D, Hyun JH, Jung K, Hannan P, Kwon HB. A calcium- and light-gated switch to induce gene expression in activated neurons. Nat Biotechnol 2017.
94. Wang W, Wildes CP, Pattarabanjird T, Sanchez MI, Glober GF, Matthews GA, *et al.* A light- and calcium-gated transcription factor for imaging and manipulating activated neurons. Nat Biotechnol 2017, 35: 864–871.
95. Harper SM, Neil LC, Gardner KH. Structural basis of a phototropin light switch. Science 2003, 301: 1541–1544.
96. Barnea G, Strapps W, Herrada G, Berman Y, Ong J, Kloss B, *et al.* The genetic design of signaling cascades to record receptor activation. Proc Natl Acad Sci U S A 2008, 105: 64–69.
97. Glazewski S, Bejar R, Mayford M, Fox K. The effect of autonomous alpha-CaMKII expression on sensory responses and experience-dependent plasticity in mouse barrel cortex. Neuropharmacology 2001, 41: 771–778.
98. Dragunow M, Faull R. The use of c-Fos as a metabolic marker in neuronal pathway tracing. J Neurosci Methods 1989, 29: 261–265.
99. Labiner DM, Butler LS, Cao Z, Hosford DA, Shin C, McNamara JO. Induction of c-fos mRNA by kindled seizures: complex relationship with neuronal burst firing. J Neurosci 1993, 13: 744–751.
100. Kovacs KJ. c-Fos as a transcription factor: a stressful (re)view from a functional map. Neurochem Int 1998, 33: 287–297.
101. Kleim JA, Lussnig E, Schwarz ER, Comery TA, Greenough WT. Synaptogenesis and FOS expression in the motor cortex of the adult rat after motor skill learning. J Neurosci 1996, 16: 4529–4535.
102. Bhat RV, Baraban JM. High basal expression of Zif268 in cortex is dependent on intact noradrenergic system. Eur J Pharmacol 1992, 227: 447–448.
103. Freed PJ, Yanagihara TK, Hirsch J, Mann JJ. Neural mechanisms of grief regulation. Biol Psychiatry 2009, 66: 33–40.
104. Belova MA, Paton JJ, Salzman CD. Moment-to-moment tracking of state value in the amygdala. J Neurosci 2008, 28: 10023–10030.
105. Matsumoto M, Hikosaka O. Two types of dopamine neuron distinctly convey positive and negative motivational signals. Nature 2009, 459: 837–841.